CHALMERS

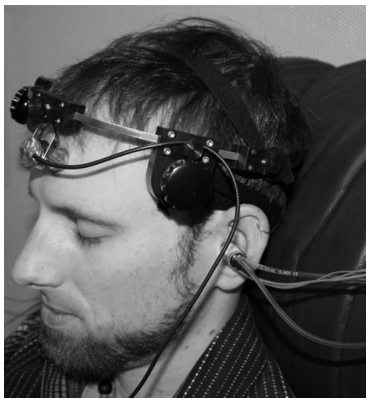

Bone-Conducted Ultrasonic Hearing:

Can Distortion Product Otoacoustic Emissions Confirm Cochlear Involvement?

Master's Thesis in the Master's programme in Sound and Vibration

JENNIFER A. MARTIN

Department of Civil and Environmental Engineering
Division of Division of Applied Acoustics
Room Acoustics Group
CHALMERS UNIVERSITY OF TECHNOLOGY
Göteborg, Sweden 2011
Master's Thesis 2011:18

MASTER'S THESIS 2011:18

Bone-Conducted Ultrasonic Hearing:

Can Distortion Product Otoacoustic Emissions Confirm Cochlear Involvement?

Master's Thesis in the Master's programme in Sound and Vibration

JENNIFER A. MARTIN

Department of Civil and Environmental Engineering
Division of Division of Applied Acoustics
Room Acoustics Group
CHALMERS UNIVERSITY OF TECHNOLOGY
Göteborg, Sweden 2011

Bone-Conducted Ultrasonic Hearing:
Can Distortion Product Otoacoustic Emissions Confirm Cochlear Involvement?

Master's Thesis 2011:18
Department of Civil and Environmental Engineering
Division of *Applied Acoustics*
Room *Acoustics Group*
Chalmers University of Technology
SE-412 96 Göteborg
Sweden
Telephone: + 46 (0)31-772 1000

Cover:
Left: Subject being tested during this study (see 5.2 Test Procedure),
Right: Photograph of cochlea
(http://www.bionicear-europe.com/en/hearing-loss/hearing-loss.html)

Chalmers Reproservice / Department of Civil and Environmental Engineering
Göteborg, Sweden 2011

Bone-Conducted Ultrasonic Hearing:
Can Distortion Product Otoacoustic Emissions Confirm Cochlear Involvement?
Master's Thesis in the Master's programme in Sound and Vibration

JENNIFER A. MARTIN
Department of Civil and Environmental Engineering
Division of Division of *Applied Acoustics*
Room Acoustics Group
Chalmers University of Technology

ABSTRACT

Human bone-conducted ultrasonic hearing is a known phenomenon in which vibrations at frequencies greater than 20 kHz, above the upper limit of human hearing, can be heard when conducted through bones in the skull. This occurrence goes against our traditional understanding of audiological processes. Many theories have been put forward and tested since the early 1950s in an attempt to explain what allows these signals to be heard. This project takes a new approach to investigating human bone-conducted ultrasonic hearing, using otoacoustic emissions measurements. These non-invasive, objective measurements are often used in clinical audiological settings. Distortion product otoacoustic emissions were elicited in test subjects via acoustic stimuli, and measured in the absence and presence of a 30-kHz bone-conducted ultrasonic signal. Any impact on the perception of acoustic stimuli, or on otoacoustic emissions produced, would help to localize where in the auditory path the ultrasonic signal was being received and processed.

Results obtained from normal-hearing ears universally showed suppression of distortion product otoacoustic emissions in the presence of bone-conducted ultrasound, at frequencies near the test subjects' upper limit of hearing. Because otoacoustic emissions are created within the cochlea by the outer hair cells, these results implicate the cochlea in the perception of bone-conducted ultrasound. Increasing the intensity of the ultrasonic masking signal resulted in a wider band of suppressed emissions, indicating a broadening of vibration along the basilar membrane.

Key words: Hearing, ultrasonic, otoacoustic emission, cochlea, bone-conduction.

Contents

Preface

This study was sponsored by the Hearing and Speech Laboratory of the Department of Otolaryngology at the University of California, Irvine, USA, under the direction of Dr. Fan-Gang Zeng. The testing itself took place in the Auditory Physiology & Psychoacoustics Laboratory at San Diego State University, California, with the support of lab director Dr. Laura Dreisbach Hawe. The ultrasonic transducer equipment was assembled and provided by Dr. Gary Sokolich, an independent audio consultant in Newport Beach, California.

The study setup was carried out in collaboration with Benjamin Sheffield, staff research associate at UC Irvine. However, this written report and most of the final testing were solely the responsibility of this author.

Acknowledgements

This project would not have been possible without the help and support of the following people:

Dr. Zeng at UC Irvine was kind enough to welcome me into his lab and suggest that I collaborate on this very interesting project. I am especially grateful to him for this opportunity, and for his advice and support.

Ben Sheffield's experience and enthusiasm were incredibly valuable in introducing the project to me and in helping to get the testing going.

Dr. Dreisbach was also very helpful; both by allowing the use of her lab, and by her dependable assistance with setup and equipment issues. Her friendly encouragement and interest in the project's success was greatly appreciated.

My advisor at Chalmers, Dr. Mendel Kleiner, was always very kind and supportive, and extremely understanding of my long-distance situation and my schedule.

Finally, I am very grateful to my husband, Graham Roff, for his patient support and encouragement throughout this project.

Thanks to all!

San Diego, June 2011

Jennifer A. Martin

Notations and Abbreviations

BCU	Bone-conducted ultrasound
DPOAE	Distortion Product Otoacoustic Emissions
DP-gram	Graph showing DPOAE results for a range of stimuli
f_1, f_2	Airborne stimulus frequencies in DPOAE testing
f_{dp}	DPOAE frequency
L_1, L_2	Airborne stimulus intensities in DPOAE testing
OAE	Otoacoustic Emissions
SL	Sensation Level
TEOAE	Transient Evoked Otoacoustic Emissions

1 Introduction and Background

When an electroacoustic transducer vibrating at an ultrasonic frequency is held in contact with the human head, a bone-conducted tone is commonly perceived by the human subject. This contradicts the traditional understanding of audiological processes, which would not allow the perception of frequencies greater than 20 kHz.

This project is an investigation into the phenomenon of human bone-conducted ultrasonic hearing using the standard audiometric measurement of distortion product otoacoustic emissions. A proper understanding of the concepts of hearing, bone conduction, ultrasound and otoacoustic emissions is necessary to appreciate the content of this study. These explanations follow.

1.1 Normal hearing

The physiological process by which sound waves enter the ear and are transmitted to the brain is shown in Figure 1. In a fully functional ear, sound pressure waves enter the ear canal and cause the eardrum to vibrate. These vibrations are transmitted to the small bones of the middle ear, known as the ossicles. In this way, pressure waves become mechanical vibrations. From there, the impedance of airborne sounds is matched to the higher impedance of inner ear fluid, and the vibrations enter the oval window, which is the entrance to the inner ear.

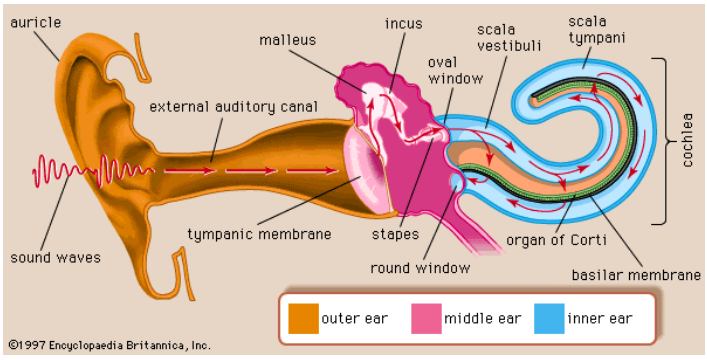

Figure 1 *Standard audiological pathway for airborne sound (Encyclopaedia Britannica, 1997)*

The inner ear is composed of the vestibular system, used for balance, and the cochlea, used for hearing. The spiral-shaped cochlea is filled with fluid and contains the basilar membrane along its entire length. The base of the basilar membrane, near the oval window, is stiff, while the apex at the opposite end is flexible. The vibrations that enter via the oval window travel along the basilar membrane and are detected via hair cells lining the membrane. The basilar membrane is tonotopic, in other words the sound waves travelling along it are detected at frequency specific locations, due to the gradient in stiffness and shape of the membrane from base to apex. The stiff base is responsible for the perception of high frequencies near the upper limit of human hearing (up to 20 kHz). The apex is responsible for the lowest frequencies around 20 Hz. Figure 2 illustrates this characteristic of the basilar membrane.

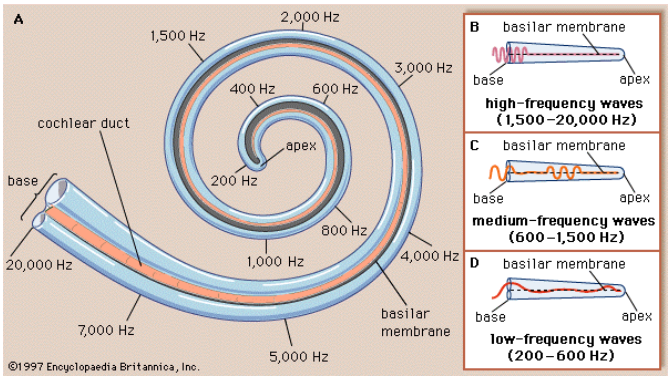

Figure 2 *Tonotopic layout of the basilar membrane (Encyclopaedia Britannica, 1997)*

There are three rows of outer hair cells and one row of inner hair cells along the length of the basilar membrane (see Figure 3). The outer hair cells are found along the more moveable centre of the membrane, while the inner hair cells are located near the anchored inner edge of the membrane. The outer hair cells can thus move and respond to stimulus much more readily. They move actively, as well as passively, in response to vibrations, as defined by their characteristic property of electromotility. The tectorial membrane, which covers the rows of inner and outer hair cells, is firmly linked to the stereocilia (hair bundles) at the tips of the outer hair cells. The inner hair cells do not make contact with the tectorial membrane.

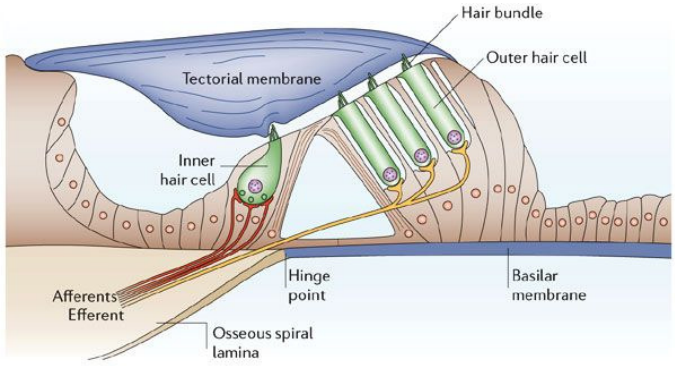

Figure 3 *Cross-section of the cochlea (Fettiplace and Hackney, 2006)*

The inner hair cells, the outer hair cells and the brain form an electromechanical feedback loop. The inner hair cells send signals to the brain via afferent fibres of the auditory nerve, while the outer hair cells receive signals from the brain via efferent nerve fibres. When a sound wave travels along the basilar membrane, the inner hair cells just barely respond, due to their location on the unmoveable part of the basilar membrane. When the brain receives the very small signal being generated by the scarcely moving inner hair cells, it sends a request via efferent nerve fibres to the outer hair cells, requesting amplification. The outer hair cells respond to the incoming sound waves by vibrating and changing shape. This increased motion causes the attached tectorial membrane to move, pulling it toward and making contact with the inner hair cells. This stimulates movement of the inner hair cells, and the information

is sent to the brain. If the signal is still not intense enough for the brain to perceive, it will send another request. In this way, the movements of the basilar membrane are accentuated in amplitude and frequency resolution and transmitted to the inner hair cells and on to the brain. For this reason the outer hair cells are often known as "cochlear amplifiers".

1.2 Bone-conducted hearing

When a vibrating object makes contact with the human head, the vibrations can travel through the bones of the skull directly to the inner ear, allowing a perception of sound as the basilar membrane vibrates synchronously. A typical example of bone conduction would be an oscillating tuning fork held to the forehead. The air-conducted sound of the vibrating object may often be heard simultaneously as it travels through the air into the outer and middle ear in the traditional way.

The bone-conducted signal bypasses the middle ear and any shortcomings it may have. For example, a bone-anchored hearing aid uses bone conduction to enable sufferers of conductive middle-ear hearing loss to perceive sound.

1.3 Ultrasonic hearing

The healthy, young human ear can normally detect sound waves that range from 20 Hz to 20 kHz, and never higher than 24 kHz (Lenhardt, 1991), although this upper limit decreases gradually with age and exposure to noise. Sound waves with frequencies above this range are known as ultrasonic, and cannot be heard by humans. It has traditionally been assumed that the human audiological system is not designed to respond to these high-frequency sounds. The impedance-matching function of the middle ear, necessary to transmit sounds from the outer to the inner ear, is known to be unable to handle ultrasonic frequencies (Pumphrey, 1950). Many animals can hear much higher frequencies than 20 kHz; cats can hear over 60 kHz, dolphins can hear up to 150 MHz.

Human bone-conducted ultrasonic hearing is a phenomenon in which vibrations even greater than 20 kHz are perceived by humans when conducted through bones in the skull. Normally this is achieved via a transducer applied to the mastoid or the forehead. This phenomenon has been reported since the early 1950s (Deatherage, 1954). When subjects are asked to match this perceived tone to an audible pitch, they generally choose a frequency between 13 and 16 kHz, or the highest frequency they can hear. Those subjects who have high frequency hearing loss will often still detect a sound, although the intensity may need to be increased to allow perception (Lenhardt, 1991).

Many theories have been put forward over the years and tested in an attempt to explain what allows these signals to be heard. The following published studies present different theories behind human bone-conducted ultrasonic hearing.

1.4 Theories about ultrasonic hearing

1.4.1 Non-cochlear receptor

Lenhardt (1991) showed that some frequency discrimination was possible in bone-conducted ultrasonic hearing, allowing for an amplitude-modulated speech signal to be carried on an ultrasonic frequency and understood by test subjects, including subjects with hearing loss. These were promising findings for potential applications in hearing devices. As for the audiological process allowing this to occur, he suggested two possibilities: either a portion of the cochlea is designed to receive these high frequencies directly, and they are sent to the brain in the traditional way, or some part of the inner ear outside the cochlea, such as the saccule, is sensitive to these frequencies over 20 kHz and transmits the information to the brain. He chose to support the latter theory, claiming that the former would not explain the ability of those with high frequency hearing loss to perceive these ultrasonic vibrations.

1.4.2 Transmission-path sound generation

Dobie and Wiederhold (1992) refuted Lenhardt's suggestion that some non-cochlear ultrasonic reception site and non-traditional auditory pathway were being used to perceive ultrasonic frequencies. They stated that the ultrasonic signal must be demodulated by nonlinearity along the transmission path, and then transduced normally by the cochlea at an audible-range frequency. They are not the first to suggest the idea that audible sounds are being generated; Haeff and Knox (1963) also performed studies of ultrasonic perception and hypothesized that sounds in the audible range were being created by resonance within the body or by imperfections in the ultrasonic transducer. Dieroff and Ertel (1975) made a strong case for demodulation as well.

1.4.3 Basilar membrane vibration

More recently, Nishimura (2003) published an extensive investigation into the ability of ultrasound to mask high-frequency air-conducted sounds. Eight normal-hearing subjects were recruited and their hearing thresholds measured between 8 and 18 kHz. These measurements were then repeated in the presence of a bone-conducted 30-kHz ultrasonic masking tone generated at levels of 5 dB SL and 10 dB SL, where SL is the sensation level that was obtained prior to testing.

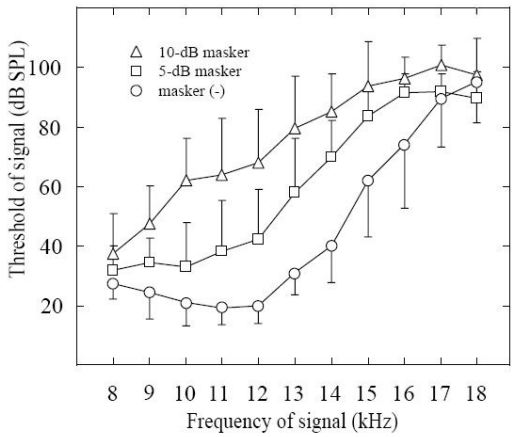

Figure 4 *Results of study by Nishimura (2003): Average hearing thresholds in the presence of ultrasonic masking at different levels. The circles represent thresholds without ultrasonic masking.*

In the presence of the 5-dB masker, the thresholds increased for nearly all frequencies, with the greatest shift of 30 dB seen at 14 kHz. With the 10-dB masker, the thresholds increased even more, especially for the lower frequencies, with the greatest shift of approximately 47 dB seen at 12 kHz. This is better illustrated in the next figure, which presents the amount of masking as a function of frequency.

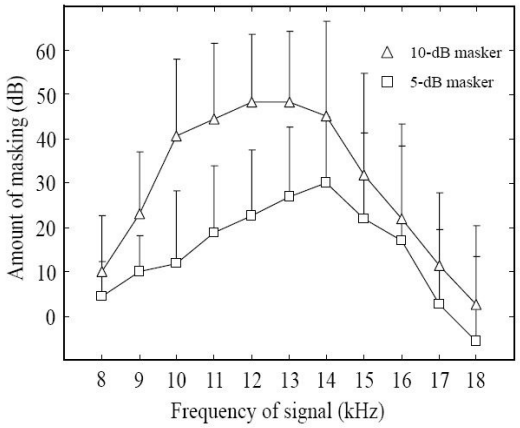

Figure 5 *Results of study by Nishimura (2003): Average amounts of masking produced by a 30-kHz ultrasonic masker at 5- and 10-dB SL.*

Nishimura pointed out that the effect of masking is strongest at the frequencies known to correspond to the normally perceived pitch of bone-conducted ultrasound (8-16 kHz) and to the upper limit of hearing. He also observed that the masking appears to extend to the lower frequencies with increased ultrasonic masker intensity. He concluded that ultrasonic hearing occurs when ultrasonic vibrations are transmitted directly to the inner ear via bone conduction, causing the base of the basilar membrane to vibrate. Given adequate signal intensity, these vibrations of the basilar

membrane will spread downward toward the apex, allowing hair cells to respond that are designed to normally pick up audible-range vibrations.

1.5 Otoacoustic emissions

Otoacoustic emissions (OAEs), discovered in 1978 by Dr. David Kemp, are low-level sounds in the ear canal produced by the vibration of the outer hair cells in response to sounds entering the cochlea. As explained in 1.1, the outer hair cells move actively in response to stimuli; this electromechanical feedback serves to selectively amplify and tune the vibrations on the basilar membrane. While this process contributes to the signal being picked up by the inner hair cells and perceived by the brain, the same vibrations are also transmitted back out the ear canal as sound waves, via the eardrum. These sounds are usually too low to be audible, but can be measured with custom instrumentation.

According to Kemp, the presence of otoacoustic emissions in an individual is an indication of healthy hearing. The frequency at which an OAE can be measured is more important than the specific intensity of that OAE, since measurement setup can have an impact. A change in OAEs in a particular individual is an indication of a change in cochlear function, but differences in OAE intensity between subjects cannot be compared. An ear with damaged outer hair cells (but working inner hair cells) will normally lose measurable OAEs, whereas an ear with damaged inner hair cells (but working outer hair cells) may still have measurable OAEs. Loss of OAEs does not necessarily indicate a loss of hearing, but rather a loss of amplitude and frequency selectivity. Likely there are other parts of the ear that are involved as well, but the outer hair cells take on the principal role in generating OAEs.

1.5.1 Measurement

Otoacoustic emissions can be measured using a probe microphone inserted into the ear canal. The test is non-invasive and objective, not requiring any interaction from the test subject. Otoacoustic emissions measurements are standard audiological tools used in clinical hearing tests, especially on infants. The subject must have a working, healthy middle ear, as the detection of OAEs can be affected by conductive losses. Typically these measurements are taken in response to a particular stimulus: Transient Evoked Otoacoustic Emissions (TEOAEs) normally make use of a click stimulus; Distortion Product Otoacoustic Emissions (DPOAEs) involve two separate continuous tones as stimuli.

The two stimuli used in DPOAEs are pure sinusoidal tones at two different frequencies, f_1 and f_2, and two different sound pressure levels, L_1 and L_2. The combination of these two tones in the ear generates otoacoustic emissions at other frequencies, known as distortion product tones. These combinations, which can often be heard by the test subject, are the result of non-linear intermodulation of the two tones, and the resulting distortion products are known to satisfy the formula $f_{dp} = f_1 + N(f_2-f_1)$ (Kemp, 2002). The ratio between f_1 and f_2 and the individual levels of L_1 and L_2 must be selected prior to testing to obtain maximum DPOAE levels. Several combinations of sound levels and frequency ratios can be effective; in general L_2 is almost always chosen to be higher than L_1 and f_2/f_1 is usually 1.2. The most prominent DPOAE is usually found at $f_{dp} = 2f_1-f_2$. Due to this known relationship

between the input and output frequencies of DPOAEs, these emissions are more helpful than TEOAEs for studying the tonotopic function of the cochlea.

1.5.2 Suppression

The suppression of otoacoustic emissions is analogous to psychoacoustic masking of audible stimuli (Kemp, 2002). In other words, a tone that masks a stimulus tone will also suppress the otoacoustic emissions normally generated in the presence of that stimulus. This means that emissions will be suppressed for frequencies at or close to the masking tone frequency. In keeping with the analogy to psychoacoustic masking, suppression contours have a similar shape to psychoacoustic tuning curves.

1.5.3 Plotting

When measuring DPOAE values of a subject, it is normally desirable to obtain the results for a range of f_1 and f_2 values. For example, a test might measure the sound level of the emission at $f_{dp} = 2f_1-f_2$ generated when f_2 = 2, 4, 6, 8 and 10 kHz, with a constant relationship between f_2 and f_1. The results are then plotted on a graph known as a DP-gram, shown in Figure 6. For each value of f_2 along the x-axis, the sound pressure level of the DPOAE at $2f_1-f_2$ is plotted. In addition, the sound pressure level of the two stimulus tones is plotted.

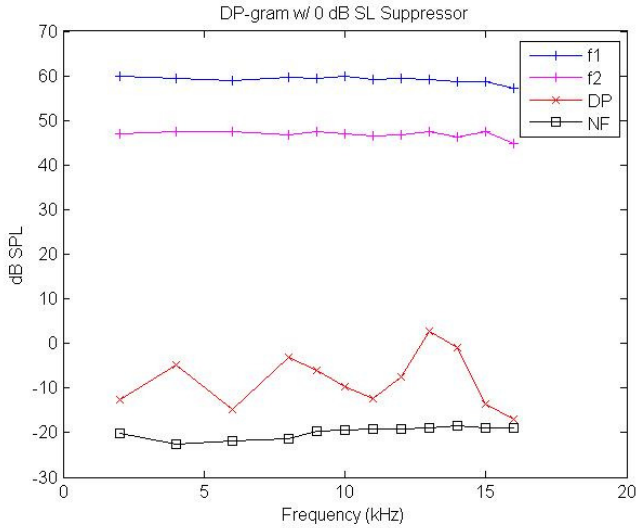

Figure 6 Example of a DP-gram.

2 Purpose

The purpose of this project was to use DPOAE measurements to better understand bone-conducted ultrasound, and to localize where in the ear the ultrasonic signal may be received and processed. DPOAE measurements should provide a view into the operations of the inner ear in the presence of bone-conducted ultrasonic vibrations. Any change in OAEs in the presence of an ultrasonic masker would indicate that the cochlea is involved in hearing it. OAEs are very stable with time as the outer hair cells do not get tired, and the repeatability is very high. DPOAEs were chosen here because, unlike TEOAEs (see 1.5.1), they are known to have frequency characteristics above 10 kHz, which is essential in this particular study since the frequency range above 10 kHz is closer to the ultrasonic range, and most likely to be affected. Another important property of DPOAEs is that when they are suppressed, the effect is similar to psychoacoustic masking, because the emission will be suppressed when the ear is stimulated at a neighbouring frequency.

Although it might seem natural to try to elicit DPOAEs using bone-conducted ultrasonic stimuli, the goal in this study was to suppress DPOAEs elicited by airborne audible-range sounds, using a bone-conducted ultrasonic masker. There are many reasons for this indirect approach. It would be challenging to generate the required levels for the two stimuli in the ultrasonic range. OAEs are produced by the outer hair cells, and ultrasonic hearing has been shown not to involve outer hair cells (Ohyama *et al*., 1985), but the cochlea may still be involved. Therefore, ultrasonic bone-conducted stimuli are not expected to elicit OAEs directly (this was confirmed by an informal test in the early days of the project). It is more likely that the effect of ultrasonic frequencies on the cochlea could be shown by measuring how DPOAEs created by air-conducted audible-range stimuli could be reduced by an ultrasonic masking tone.

By using OAEs in this manner we can better understand the cochlea's possible function in hearing bone-conducted ultrasound, allowing us to compare and clarify the current theories about bone-conducted ultrasonic hearing. If a bone-conducted ultrasonic signal, presented as a masking signal, has any impact on the perception of acoustic stimuli, or on OAEs produced, then this would help to localize where in the auditory path the ultrasonic signal is being received and processed.

3 Hypothesis

The expected outcome of this study was based on the theory presented by Nishimura about the downward spread of masking along the basilar membrane (see Section 1.4.4). The resulting assumption was that the cochlea is involved in ultrasonic hearing. Specifically, in the presence of an ultrasonic masker, the basilar membrane vibrates. Given strong enough vibrations, this allows the most basal inner hair cells, which normally respond to audible-range high frequencies, to be excited. Therefore, the expected result of this study was that the ultrasonic masking signal would have a detrimental effect on the ability to perceive the two-tone audible-range stimulus at high frequencies near the test subject's upper limit of hearing, thereby reducing the DPOAEs produced.

4 Measurement setup

In order to perform this test, each test subject had to have a small probe inserted into one of their ears, containing a microphone and two speakers, and an ultrasonic transducer mounted on a headband and pressed against their forehead. DPOAE testing requires that a two-tone stimulus be played into the ear canal, and the response in the ear be measured with the probe microphone. For this study, the test needed to be performed in the absence and presence of the bone-conducted ultrasonic stimulus at controlled, increasing sound levels. The following sections discuss the existing standard measurement equipment and available software, and explain why a new custom setup was required.

4.1 Standard otoacoustic measurement equipment

Commercial OAE units, such as the one made by BioLogic, do not allow for experimentation in the 8-16 kHz range (the range of interest for this study). For this reason, custom instrumentation was needed for this test. The custom equipment already in use by Dr. Laura Dreisbach at San Diego State University was utilized. The focus of Dr. Dreisbach's work is the measurement of DPOAEs at frequencies greater than 10 kHz, up to 16 kHz. Therefore her equipment was ideally suited to this project's testing, and has been proven to be reliable. Modifications were made to the setup to incorporate the ultrasonic transducer designed by Dr. Gary Sokolich.

4.2 Custom DPOAE lab equipment

The following equipment is used by Dr. Dreisbach to make DPOAE measurements. The external sound card is a MOTU 828 mkII audio processor with multiple inputs and outputs. The ear probe is custom-made using a pair of modified Sennheiser CX-300 earbuds. These are encased in two sealed metal cylinders, coupled to two 16-gauge medical tubes. These tubes are then connected to an Etymotic Research ER-10B+ emission probe microphone. The probe is capped with a foam probe tip and inserted into the ear, as shown in Figure 7, thus allowing two separate audio input channels and one output channel to be securely positioned in the ear canal.

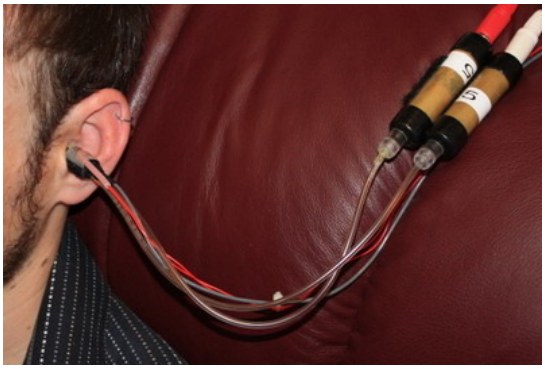

Figure 7 The DPOAE ear probe, attached via tubes to the Sennheiser earbuds

4.3 Custom Ultrasonic test equipment

In addition to the DPOAE equipment normally used in this laboratory, additional equipment was needed to create the ultrasonic tone. The ultrasonic transducer, provided by Dr. Gary Sokolich, was composed of a piezoelectric transducer capable of vibrating at frequencies between 25 and 45 kHz. The output of this transducer has been tested to ensure that it is linear and contains no subharmonics. An HP467A power amplifier plus a custom amplifier were used to power the transducer. Finally an adjustable headband was designed for this study to allow consistent positioning of the transducer on the subject's forehead.

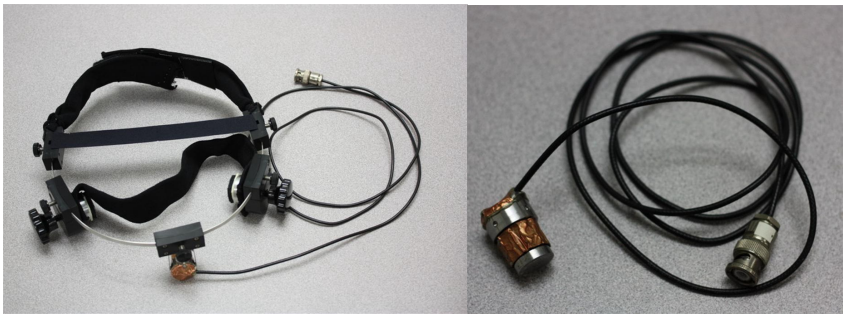

Figure 8 Ultrasonic transducer and headband

4.4 Standard test software

To run her tests and analyse the results, Dr. Dreisbach uses EMAV, a free program created by Stephen Neely and Zhiqiang Liu of Boys Town National Research Hospital for measuring and displaying otoacoustic emissions. This program does not offer the flexibility of a third stimulus channel for the ultrasonic bone-conducted signal to be presented simultaneously. In order to include the ultrasonic bone-conducted signal in the automated test procedure, a new automated test procedure was needed to present the sequence of tone pairs and ultrasonic stimuli to the listener, record the resulting otoacoustic emissions, and plot the data.

4.5 Custom software

Although EMAV is a well-established, highly dependable program for measuring DPOAEs up to 16 kHz or higher, it was not usable for this study. Firstly, it was necessary to have control of three output signals (two for the stimulus tones and one for the ultrasonic tone) while EMAV only controls two output signals. Also, the sampling frequency in EMAV is 44 kHz, which would not accommodate a 30 kHz output signal without any aliasing. In addition, more customisation was required for the timing of the tones. Therefore, an automated test procedure was created in MATLAB, with functionality based on EMAV.

The in-ear calibration portion of the EMAV test was still employed at the very beginning of the test. Once the calibration was run, the resulting calibration output data was entered into the new custom program; the remainder of the test was run by

the new program, based on this calibration data. The sampling frequency in the custom software was 96 kHz, well over the Nyquist frequency of 60 kHz.

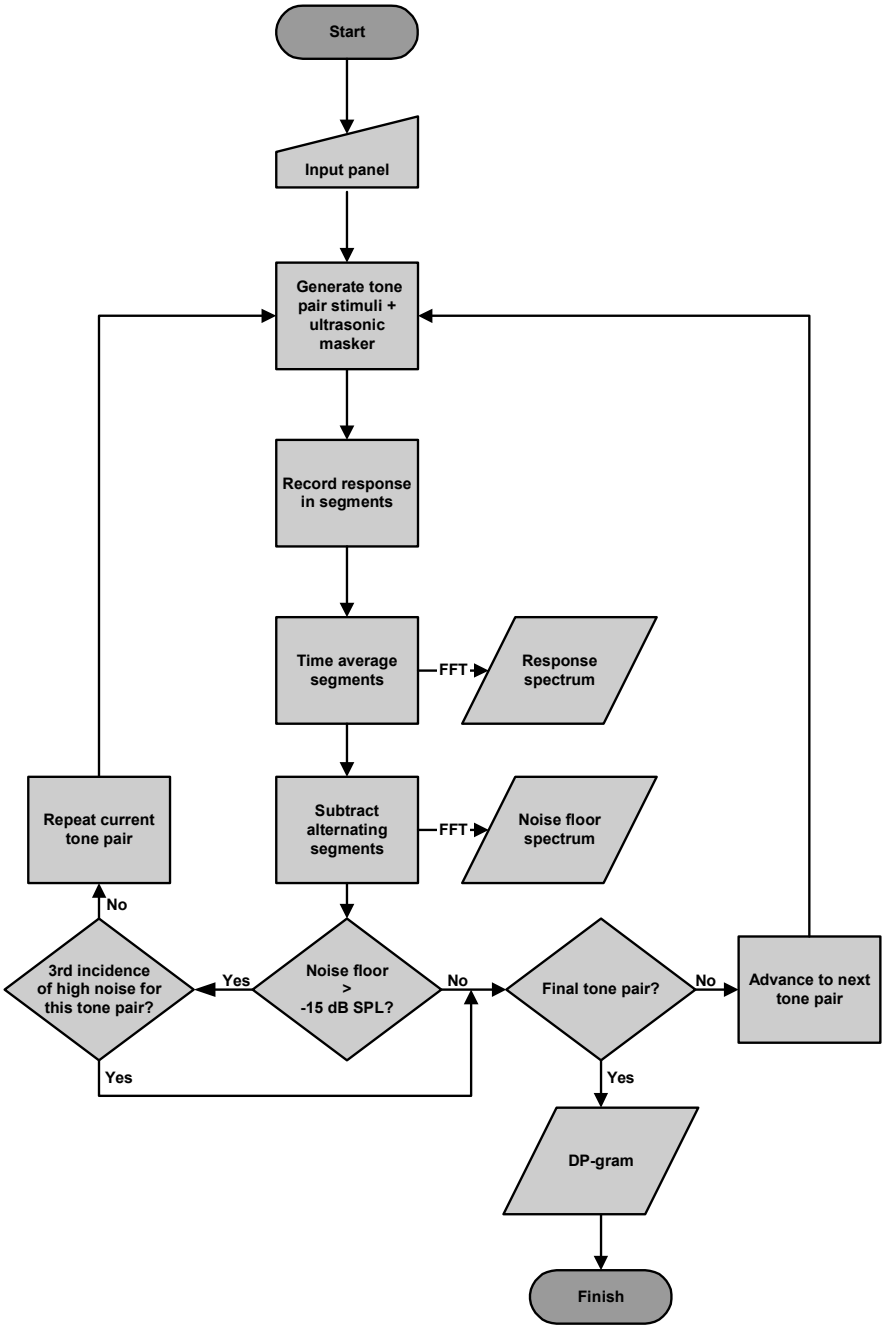

Figure 9 Outline of custom software structure

The flow chart in Figure 9 outlines the basic structure of the MATLAB code. The test begins with an input panel window, in which the test operator must enter the following information: the subject calibration data file name and the subject's dynamic range for the ultrasonic tone (the threshold and the maximum comfortable level in dB). As well, the operator must choose whether to generate an ultrasonic

signal for this round of testing, and what the level should be (0, 5, 10, 15, or 20 dB SL). Following this, the test operator clicks a button to start the test.

The first tone pair is generated, starting randomly with either f_2 = 2 kHz or f_2 = 16 kHz. For each pair of frequencies, the stimulus tones are repeated 16 times to allow for better averaging and a lower noise floor. The tone duration is 683 msec per repetition, with a 200-msec pause between tones. The ultrasonic tone, if selected, is generated simultaneously but held constant for 1.083 seconds, through the 16 tone-pair repetitions, as this was deemed to be more comfortable to the subject. (These tone durations were converted from number of samples to seconds, hence the awkward numbers.) The frequency of the ultrasonic tone is 30 kHz. There is a 15-second gap between primary pairs in order to give the test subject a short break.

The microphone probe records the response in the ear canal during the presentation of each tone pair, capturing both the computer-generated tones and any otoacoustic emissions. The recorded response is then split into 16 consecutive segments for analysis. This follows the analysis procedure suggested by Dreisbach (2001). These 16 recorded segments are averaged in time to obtain a clean response, which is then brought to the frequency domain via a Fast Fourier Transform. The result is a spectrum of the response recorded in the ear canal. It is important to compare this response to the noise floor in order to see how significant the results are. The noise floor spectrum is obtained by subtracting the sum of the odd-numbered segments of the recorded response from the sum of the even-numbered segments, dividing by 16, and then taking the Fast Fourier Transform. In this way most constant noise, such as line noise, will be reduced or eliminated. The spectra from the 16 tone pair repetitions are then averaged, and the resulting response and noise floor spectra are displayed on the computer screen. See Section 6.2, Figure 12 for an example.

The program then seeks the value of the response at $2f_1 - f_2$ to determine if there is a measurable DPOAE. The noise floor at $2f_1 - f_2$ has to be less than –15 dB SPL for the result to be valid. This value was chosen after many system trials to be the lowest possible for this system. If the noise floor is acceptable, the value of the response is recorded as the DPOAE for that tone pair, and displayed on the DP-gram on the screen. If the noise floor is too high, the test starts over for that tone pair. To avoid endless repetitions, the test will repeat only once for each tone pair, and then will skip to the next tone pair, and no DPOAE is displayed on the DP-gram for that tone pair. When the final tone pair is complete, the complete DP-gram is displayed and recorded (as seen in Figure 6).

5 Test description

5.1 Test subjects

Test subjects had to have healthy ears, normal hearing and robust high-frequency DPOAEs in order to be candidates for this study.

For each potential subject, both ears were examined and tested for middle ear function. Following this, a Von Békésy hearing test was administered to determine airborne hearing thresholds. Subjects needed to respond to tones at all tested frequencies from 1 through 16 kHz, with thresholds ideally below 30 dB SPL for the range of 1 to 8 kHz. If a subject's thresholds were slightly outside this limit, they could still qualify for the study if they had strong DPOAEs, as confirmed in the next step of the screening.

Subjects were then screened for the presence of DPOAEs at $2f_1-f_2$ for values of f_2 from 16 kHz down to 1 kHz, in 1 kHz decrements. The frequency ratio (f_2/f_1) was always 1.2 and the levels of the frequency primary tones were 57 and 45 dB SPL. The stimulus levels were determined by an in-the-ear calibration procedure conducted at the beginning of the test. In order to qualify for the test, the DPOAEs had to be at least 5 dB above the noise floor at 2 through 8 kHz, and there had to be at least five frequency points with measurable DPOAEs between 9 and 16 kHz.

Following this screening, 5 candidates were accepted for the study. Some candidates had only one qualifying ear, resulting in 8 ears confirmed for the study. All candidates were between the ages of 20 and 31; there were 5 female ears and 3 male ears.

The hearing thresholds for all accepted subjects are shown in Figure 10. Baseline DPOAE levels for all subjects are shown in Figure 12 in Section 6.1.

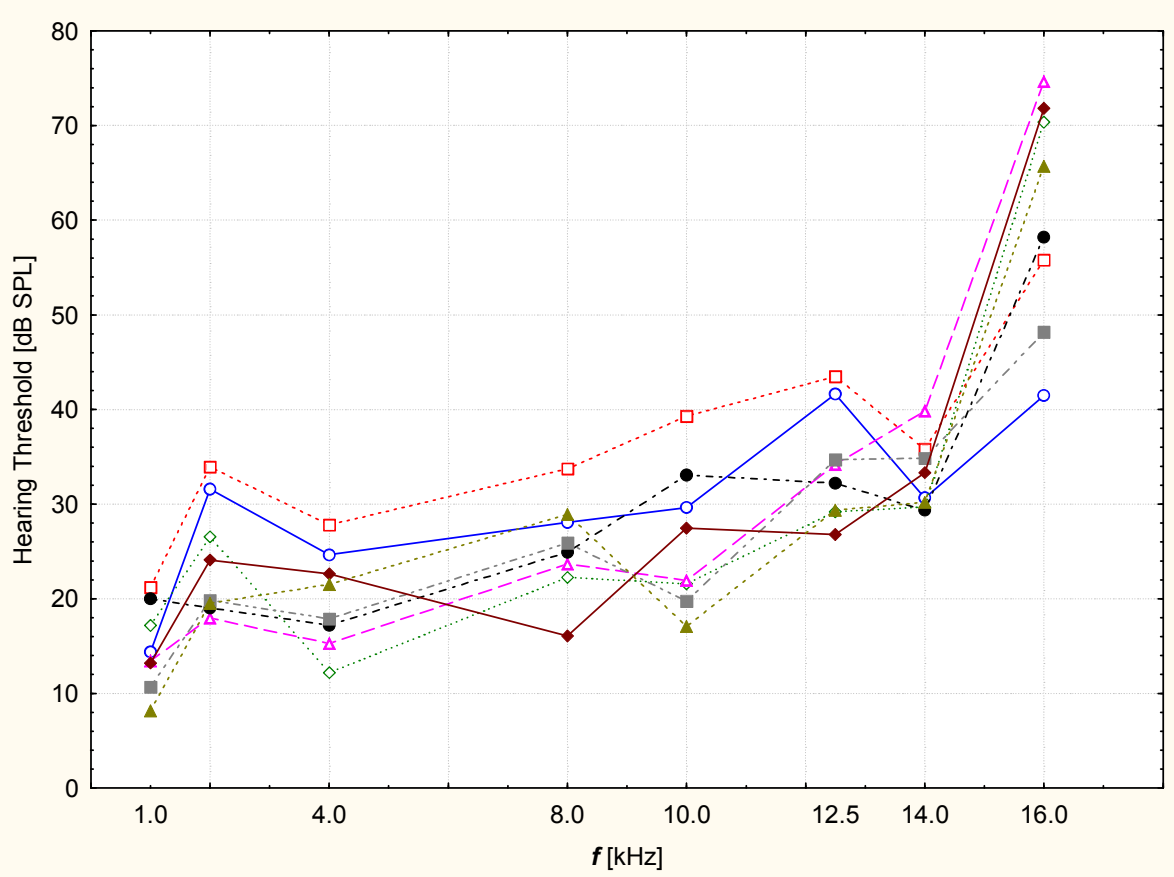

Figure 10 Combined hearing thresholds for all eight chosen candidate ears

The one subject with thresholds approaching 35 dB SPL for 2 and 8 kHz, seen as the top line in Figure 10, was deemed an acceptable candidate after demonstrating very strong DPOAEs in the 9 to 16 kHz range.

5.2 Test procedure

When one or both ears met the study criteria, the test commenced immediately. The subject was given the ultrasonic transducer and asked to find the location on their forehead at which the transducer would create a robust bone-conducted tone perceived in the ear being studied. The headband was then attached securely to the subject's head to ensure that the transducer would remain in this location throughout the testing. In order to determine the subject's threshold and dynamic range, ultrasonic tones were generated at incrementally decreasing and increasing levels, much like a regular hearing test. The subject identified their maximum comfort level, with 20 dB SL being the maximum level that was presented.

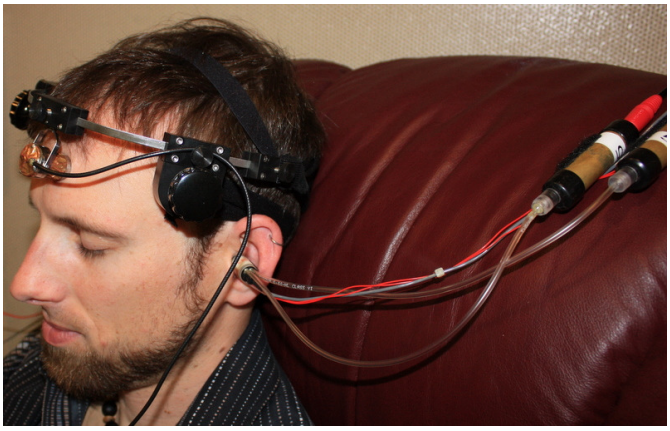

Figure 11 *A test subject ready to begin, with ear probe, headband, and ultrasonic transducer in place.*

A series of DPOAE tests were then performed on each subject using the new MATLAB automated test procedure. DPOAEs were measured for primary tone pairs at f_2 = 2, 4, 6, 8, 9, 10, 11, 12, 13, 14, 15 and 16 kHz, with $f_1 = 1.2f_2$. The entire test sweep was performed up to five times, depending on the subject's dynamic range, for ultrasonic signal levels of 0, 5, 10, 15 and 20 dB SL (in varying order). L_1 and L2, the levels of the f_1 and f_2 tones, respectively, were kept at L_1=57 dB SPL and L2 = 45 dB SPL.

6 Results

Complete results were collected for the eight subject ears that met the stated requirements.

6.1 Baseline emissions – all subjects

The baseline DPOAEs for all eight tested ears, without bone-conducted ultrasound, are shown in a combined DP-gram below. (L1 = 57, L2 = 45, $f_1 = 1.2f_2$)

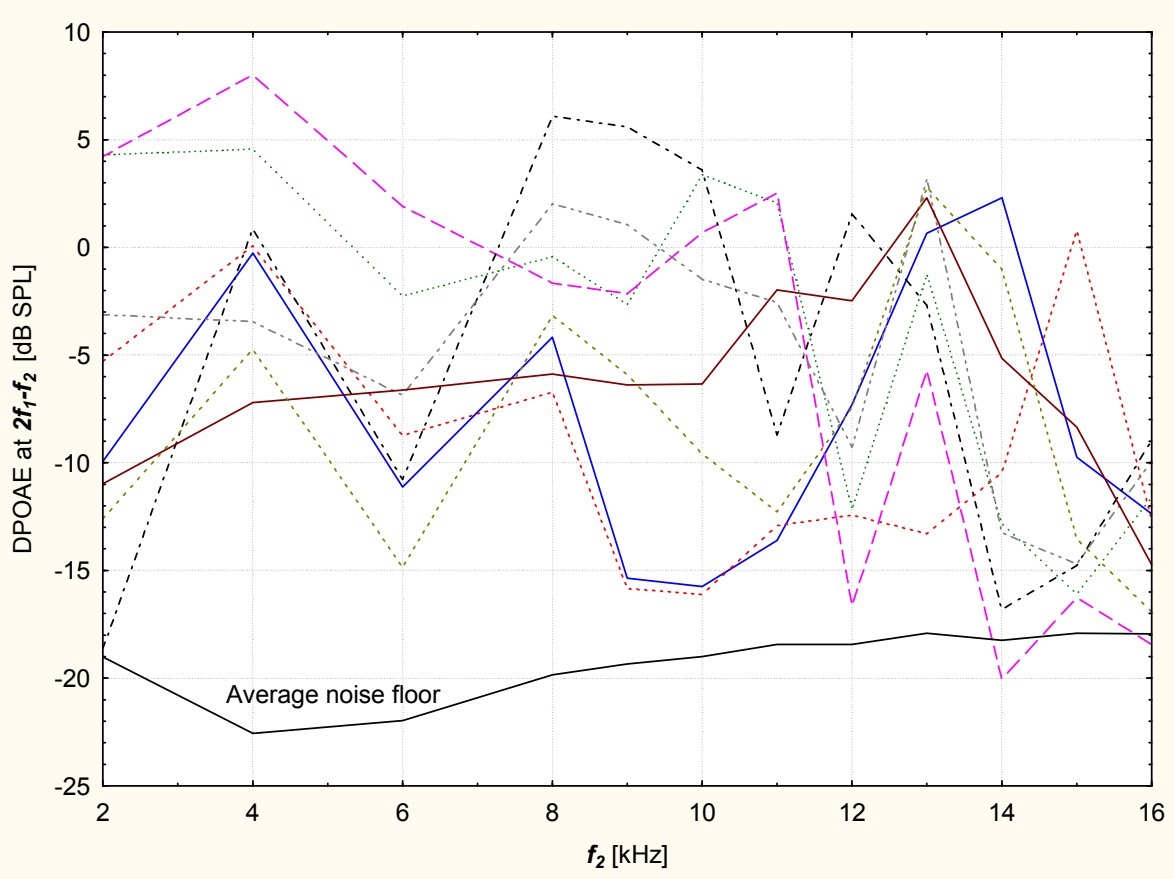

Figure 11 Subject baseline DPOAE levels for L_1 = 57 dB, L_2 = 45 dB, $f_1 = 1.2f_2$

Clearly there is great variation in otoacoustic emissions between all eight of these healthy, normal ears. At the high frequencies, it is interesting to observe that many ears have very low emissions at f_2 = 12 kHz, and a peak in emissions at f_2 = 13 kHz. Above 13 kHz, most subject's DPOAEs drop off quite quickly, although one subject had significant emissions at f_2 = 15 kHz. These results are highly repeatable for these measurement conditions with L_1 = 57 dB, L_2 = 45 dB, and $f_1 = 1.2f_2$.

6.2 Sample individual output - without ultrasound

Figure 12 shows a screenshot from the testing software with a sample frequency response as measured in a subject's ear for a set of stimuli. The two stimuli, at f_1 = 10.8 kHz and f_2 = 13 kHz, are clearly seen on this spectrum. The DPOAE can also be observed as a 2.8-dB spike at $2f_1-f_2$ = 8.6 kHz. The average noise floor is seen at approximately –20 dB.

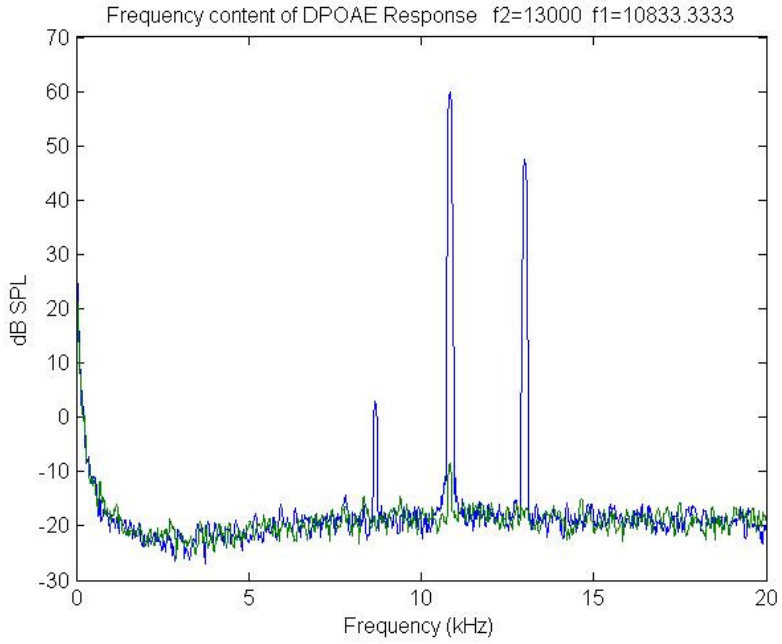

Figure 12 Sample frequency spectrum of measurement taken with no bone-conducted ultrasound

A screenshot of the resulting DP-gram for this same subject ear, as explained in Section 1.5.3 and shown in Figure 6, is repeated in Figure 13. The DPOAE of 2.8 dB from Figure 12 can be found in this DP-gram at f2 = 13 kHz.

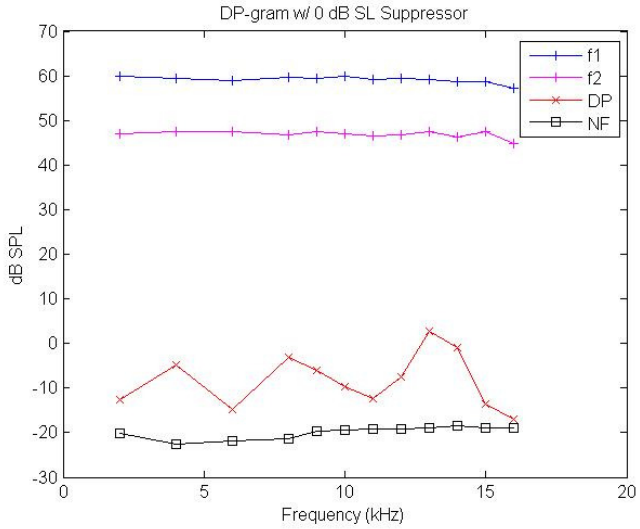

Figure 13 Sample DP-gram plotting DPOAE levels for one subject taken with no bone-conducted ultrasound

6.3 Sample individual output - with ultrasound

In the set of three figures that follow, displayed output is shown for one subject ear at three different levels of bone-conducted ultrasound. The ear probe and the ultrasonic transducer remained unmoved throughout the measurements. The stimulus tones were identical for all three measurements: Tone 1 was 12.5 kHz and 62 dB SPL, and Tone 2 was 15 kHz and 50 dB SPL.

In Figure 14a, there is no ultrasonic masker signal. The stimulus tones and the DPOAE at 10 kHz are seen clearly. In Figure 14b, the ultrasonic signal level is 0 dB SL, the subject's threshold. The 30-kHz signal is seen in the spectrum as a 40-dB spike, showing that it is present in the ear canal. However, the DPOAE is relatively unchanged from the no-ultrasound test condition. This demonstrates that an ultrasonic signal at the subject's threshold, and thus barely detectable to the subject, does not have a noticeable impact on the subject's DPOAEs. In the final figure, 14c, the ultrasonic signal level is 15 dB SL, and it is seen in the spectrum as a spike at around 55 dB SPL, which is 15 dB higher than in the previous figure. In this case the DPOAE is still there, but noticeably diminished by almost 10 dB. This agrees with the hypothesis that the ultrasonic tone would suppress the DPOAE.

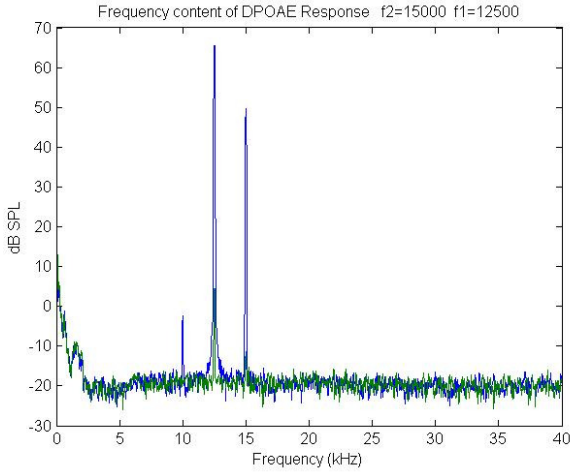

(a)

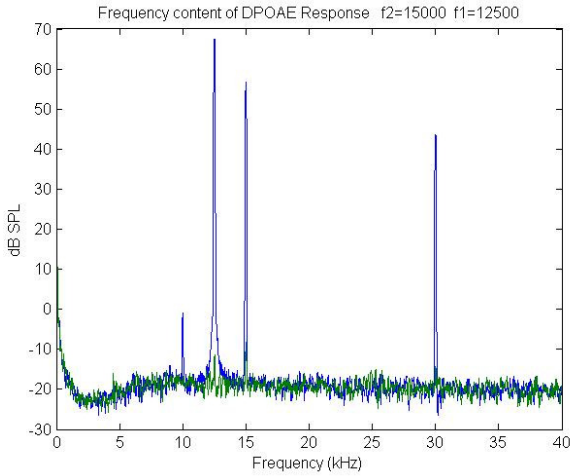

(b)

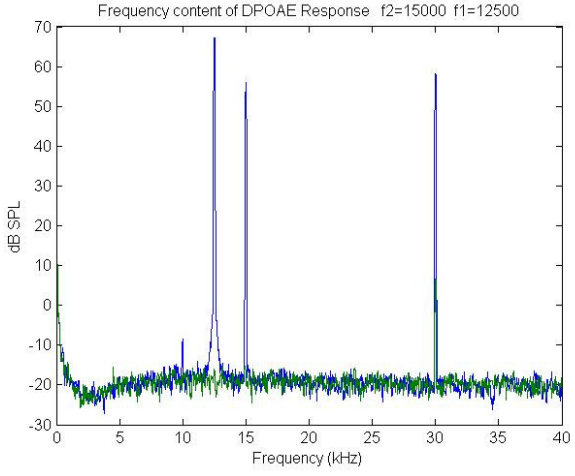

(c)

Figure 14 Sample frequency spectrum with (a) no ultrasound, (b) 0 dB SL of ultrasound, (c) 15 dB SL of ultrasound

6.4 Averaged results for all subjects

The DPOAE levels at each tested frequency pair were plotted on a DP-gram. An average DP-gram for all eight tested ears is shown in Figure 15.

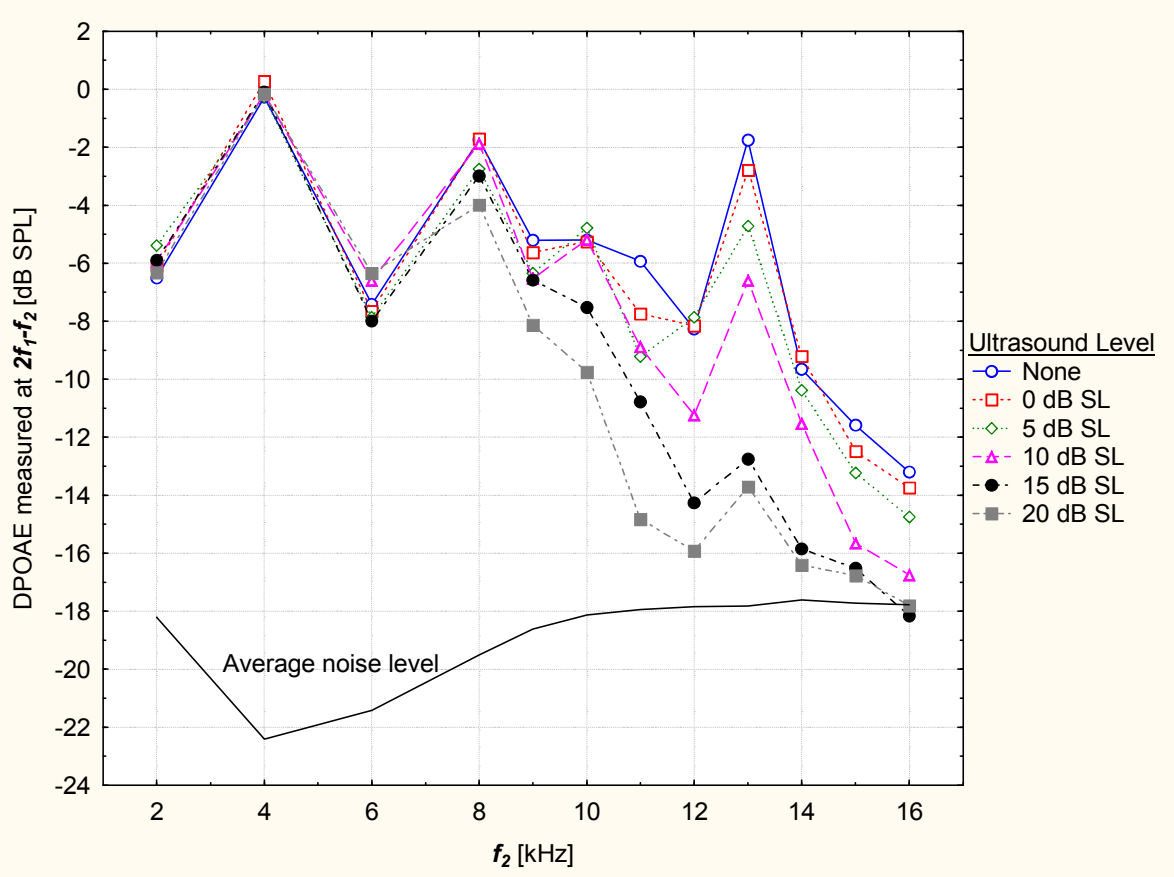

Figure 15 DPOAE levels averaged for all subjects

This figure contains 5 DPOAE curves for the five levels of ultrasonic signal: 0 through 20 dB above sensation level. Also plotted is the average noise floor. This graph shows a clear difference between the DPOAEs measured at different levels of ultrasound. In the presence of greater bone-conducted ultrasonic intensity, the strength of the measured DPOAEs at the highest frequencies (8-16 kHz) is less. In addition, this suppression of the DPOAEs increases with ultrasonic intensity, and its effects are seen at increasingly lower stimulus frequencies.

Since most subject ears showed a peak in their baseline DPOAEs (section 7.1) at 13 kHz, this peak is also seen in these averaged results.

Table 1 summarizes the average shift in DPOAE levels at every frequency for every bone-conducted ultrasound condition. Significant shifts ($p < 0.05$) are displayed in bold.

Table 1 Average DPOAE level shift in the presence of each ultrasonic masker

f_2 [kHz]	Level shift [dB SL] per masker level:				
	0 dB SL	5 dB SL	10 dB SL	15 dB SL	20 dB SL
2	0.42	1.11	0.56	0.61	0.32
4	0.54	0.00	0.10	0.17	0.10
6	-0.24	-0.45	0.82	-0.58	-0.13
8	0.03	-1.01	-0.13	-1.25	-3.03
9	-0.41	-1.14	-1.32	-1.38	-4.17
10	-0.06	0.42	0.02	-2.32	**-5.79**
11	-1.81	-3.28	**-2.95**	**-4.85**	**-9.25**
12	0.11	0.41	**-2.98**	**-6.00**	**-7.88**
13	-1.03	**-2.97**	**-4.84**	**-11.01**	**-12.46**
14	0.45	-0.73	-1.88	-6.19	**-6.74**
15	-0.90	-1.64	**-4.06**	-4.94	**-5.48**
16	-0.54	-1.56	**-3.55**	**-4.96**	**-4.44**

Significant decreases in emissions are seen at 9-16 kHz with the 20 dB SL ultrasonic tone, at 11-13 kHz and 16 kHz with 10 and 15 dB SL, and at 13 kHz with 5 dB SL. There is no significant difference between the DPOAEs measured without ultrasound and with ultrasound at the subject's threshold (0 dB SL).

6.4.1 Averaged Results: Emission Suppression

Another way to look at the results is to plot the amount of DPOAE suppression observed at different levels of bone-conducted ultrasound (the inverse of the above table). DPOAE suppression is the difference in DPOAE level when measured with and without the ultrasonic masking tone. This is shown in the following graph, with the amount of suppression as a function of stimulus frequency for different intensities of ultrasound.

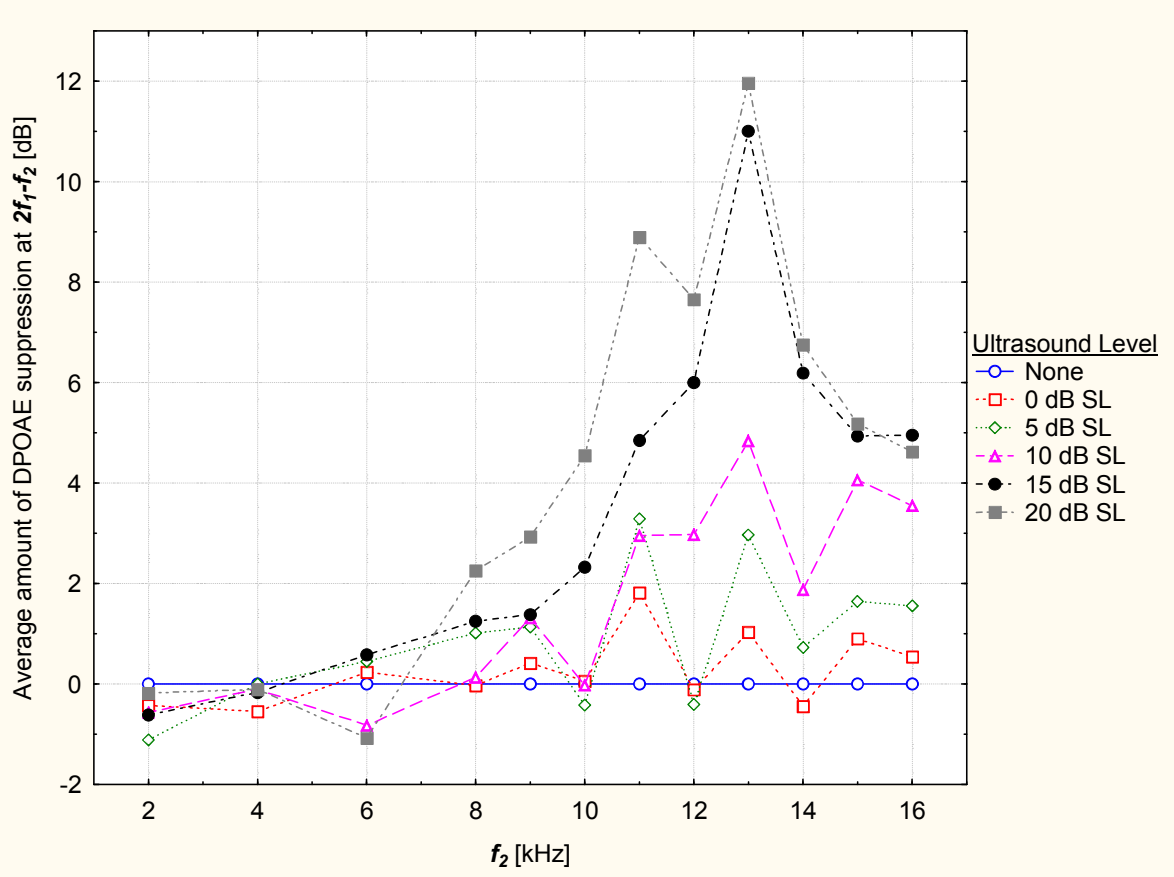

Figure 16 *Average amount of DPOAE suppression observed in the presence of each ultrasonic signal*

These results can be compared to the results obtained by Nishimura in Figure 5. The analogy between emission suppression and psychoacoustic masking is clearly demonstrated in these graphs. However, the above graph, and Figure 15, can be difficult to interpret, since the peak that most subjects had in their baseline DPOAEs at about 13 kHz is somewhat misleading. It may appear at first glance that there is a more dramatic suppression effect at 13 kHz than at 16 kHz. In reality, having greater baseline DPOAEs at 13 kHz allowed for more significant suppression. However, although the average DPOAEs at 13 kHz did experience more reduction at 20 dB SL of ultrasound, the percentage of reduction was greater at 16 kHz. For 15 and 20 dB SL, the emissions at 16 kHz have been reduced to the noise floor or lower, and thus are considered to be eliminated, or completely suppressed. A graph showing the percentage of emissions suppressed is helpful, as in Figure 17.

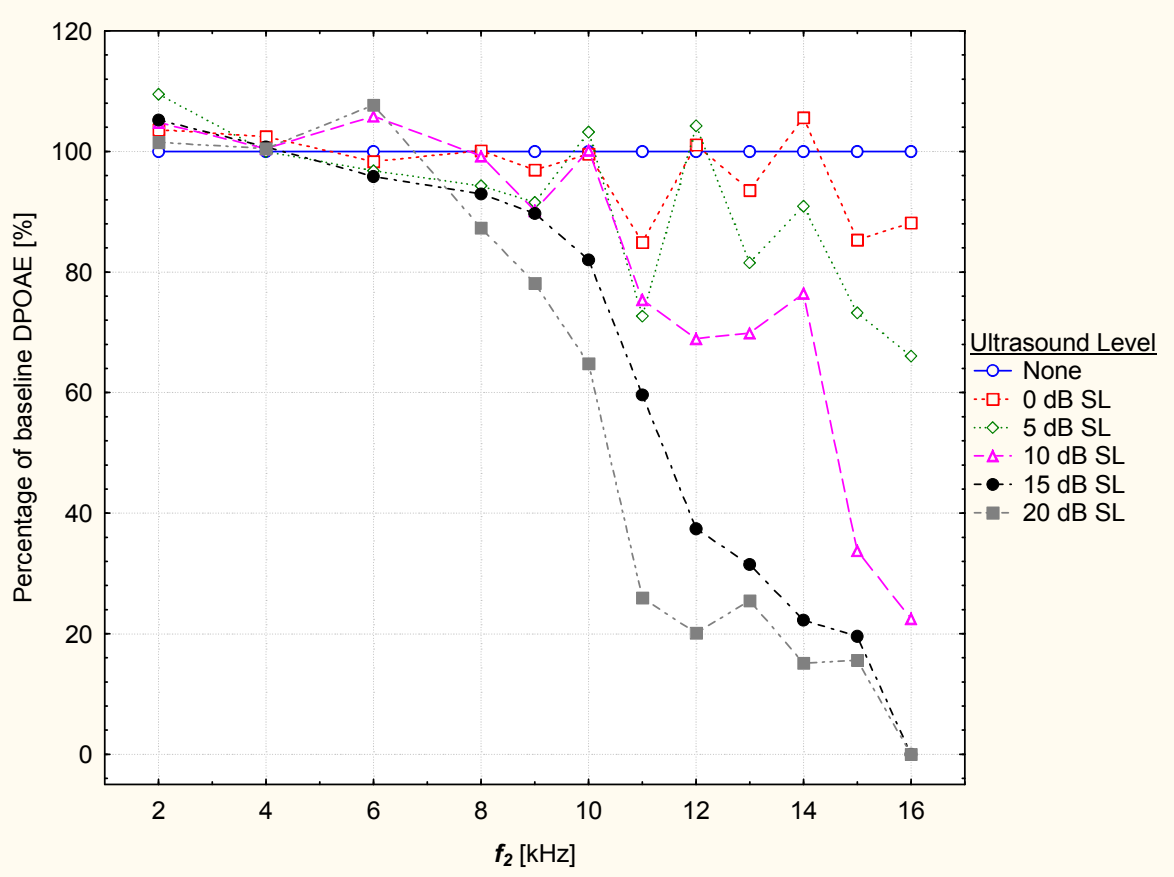

Figure 17 *Average DPOAE levels in the presence of ultrasound as a percentage of the baseline DPOAE levels*

In this graph, the average DPOAE levels without any ultrasound are considered to be 100 percent. The average DPOAEs at different levels of ultrasound are shown as percentages of the original DPOAE measurement without ultrasound. DPOAEs that were eliminated in the presence of the ultrasonic masker are plotted at 0 percent of the baseline. Points plotted above 100% are due to minor experimental error (such as accidental ear probe or headband adjustment between test cases) and are considered to be equivalent to 100% for this analysis.

This graph shows that the percentage of DPOAE suppression grows with stimulus frequency. Also seen clearly here is the increasing range of frequencies affected as the ultrasonic suppressor tone increases in intensity. The effects of suppression spread as low as 8 kHz for the condition of 20 dB SL.

6.5 Test reliability

It is important to confirm that any differences between measurements were the result of differences in measurement conditions, and not the result of an unreliable test setup. For this reason, the DPOAEs of one test subject were measured five times consecutively, without ultrasound. The results are shown in Figure 18.

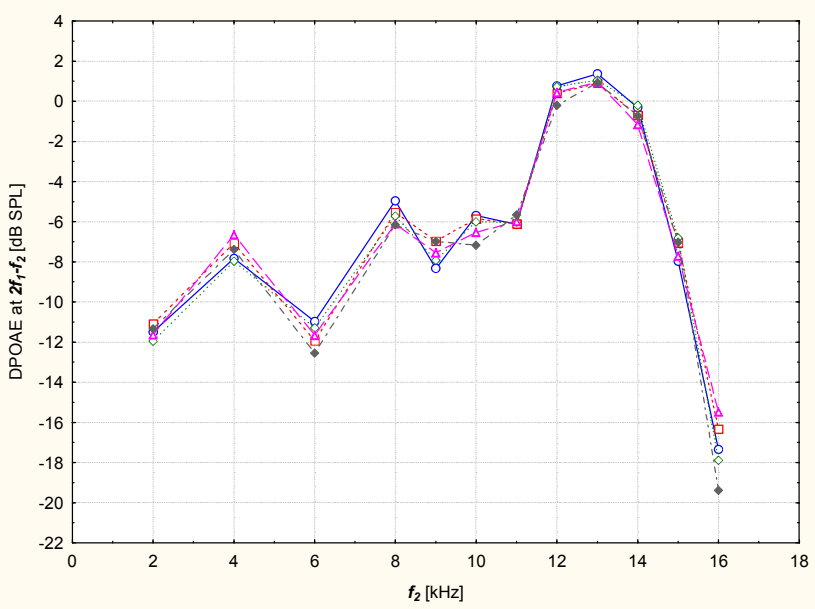

Figure 18 *A standard DPOAE test performed five times sequentially to show equipment reliability*

Visually, these five curves appear almost identical. Numerically, the reliability can be expressed in terms of three-sigma (3σ). The three-sigma rule states that for a normal distribution of results, nearly all values lie within 3 standard deviations of the mean. The three-sigma value per frequency of measurement is shown in Figure 19, along with some of the suppression curves from Figure 16 as a comparison.

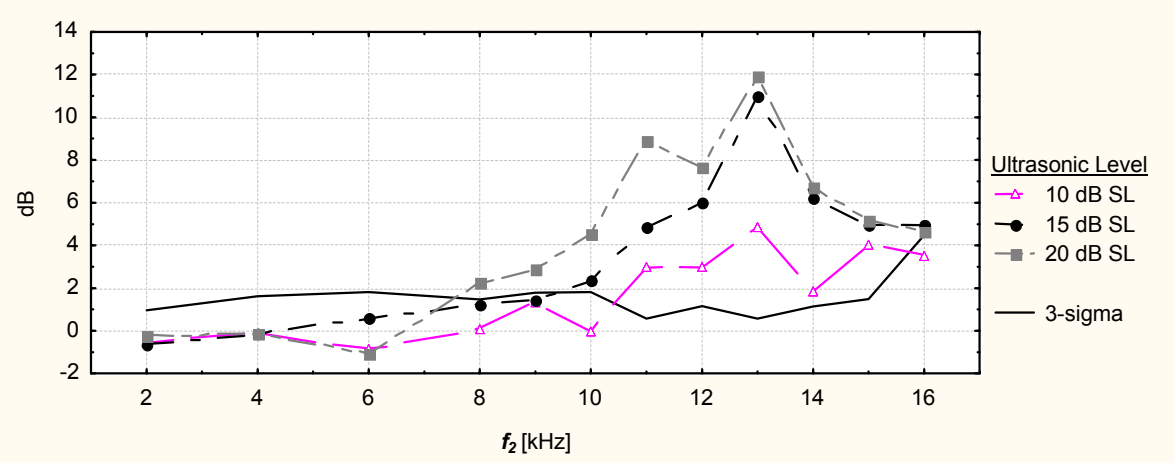

Figure 19 *3-sigma plot juxtaposed with average amount of DPOAE suppression*

In this case, the average 3σ is 1.57 dB. This indicates that nearly all values at each frequency point, on average, lie within 1.57 dB of the average. A larger drop from the mean would thus indicate a change in measurement conditions, not just test variation. This is a very small range, considering that the amount of suppression that has been

observed in this experiment is as much as 10 dB. In fact, this average 3-sigma would be even lower if the 16-kHz point were left out of the results. The 3-sigma at 16 kHz is 4.48 dB. The measurements at 16 kHz are thus the least reliable. The average 3-sigma for 2-15 kHz is 1.3 dB.

7 Discussion

These test results unquestionably show the suppression of DPOAEs created by air-conducted audible-range stimuli by the bone-conducted ultrasonic masking tone. This indicates that the cochlea was significantly involved in hearing the tone. Other parts of the ear, brain or elsewhere may also be involved, but the cochlea is a critical component in the process. If the cochlea played only a small role, or were not involved at all, and some other part of the inner ear outside the cochlea was responsible instead (as suggested by Lenhardt, 1991), these DPOAEs would not be affected by the presence of the masker.

No subharmonics of the ultrasonic signal were measured in the ear canal. See Figure 14, which shows that the two stimulus tones, the DPOAE at $2f_1-f_2$ and the pure ultrasonic tone at 30 kHz were the only tones recorded in the ear canal. This indicates that there was no measurable demodulation of the ultrasonic tone. If the ultrasonic signal were demodulated by nonlinearity along the transmission path through the head (as suggested by Dobie, R.A., Wiederhold, M.L.), then there would be noticeable subharmonics of the 30-kHz tone in the frequency content measured at the ear.

Even if there were subharmonics of the ultrasonic signal present somewhere in the head that were too low to be recorded in the ear canal, they could not account for the dramatic impact on the DPOAEs seen here. The suppression of DPOAEs observed is much more substantial than it would be with even an audible-range suppressor at such a low level. For example, Gorga and Neely et al. (2003) observed that for a stimulus pair where $\mathbf{L_2}$ is 50 dB SPL, a suppressor tone of similar frequency to $\mathbf{f_2}$ was only effective at suppressing the DPOAEs if it were above 40 dB SPL. In contrast, the bone-conducted ultrasonic tone in this study was 20 dB above sensation level at its highest, with stimulus tones of $\mathbf{L_1}$ = 57 dB and $\mathbf{L_2}$ = 45 dB.

The DPOAEs were reduced the most at the higher frequencies of 13-16 kHz, near the test subjects' upper limit of hearing. With increasing intensity, the bone-conducted ultrasonic signal masked a wider band of DPOAEs, starting with the highest frequencies and spreading downward. It is thus possible that ultrasonic vibrations do elicit vibrations of the basilar membrane, and that in the presence of an intense bone-conducted ultrasonic masker, the basilar membrane responds with strong enough vibrations that the most basal inner hair cells are excited. These inner hair cells are not designed to normally pick up frequencies above 20 kHz. However, inner hair cells can respond to sounds on their own (without the aid of the amplifying outer hair cells) if intensity is sufficiently high. The inner hair cells do not have much frequency selectivity, but as long as they are vibrating there will be a perception of sound, even if it isn't heard at the correct pitch. With increased ultrasonic intensity, a larger section of the basal end of the basilar membrane is excited.

This supports the theory of Nishimura, T. *et al* that a downward spread of vibration along the basilar membrane allows hair cells to respond that are designed to normally pick up audible-range vibrations. Ultrasonic bone-conducted stimuli do not elicit OAEs directly, meaning that ultrasonic hearing must activate inner hair cells only. These suppressed DPOAEs would then correspond to the frequencies at which the masker is perceived.

8 Conclusions

Distortion product otoacoustic emissions created by air-conducted audible-range stimuli at frequencies near the upper limit of hearing can be suppressed in humans with a bone-conducted ultrasonic signal. This confirms the involvement of the cochlea in bone-conducted ultrasonic hearing.

In addition, increasing the intensity of bone-conducted ultrasound results in increased suppression of DPOAEs over a wider range of high frequencies, indicating a downward spread of vibration along the basilar membrane. This supports the theory that perception of bone-conducted ultrasonic signals is caused by the excitation of the most basal inner hair cells due to intense vibrations of the basilar membrane.

9 Future work

This study is the first step toward a new direction of investigation into the workings of bone-conducted ultrasound. Now that it has been established that DPOAEs can be suppressed by a bone-conducted ultrasonic tone, it seems likely that further testing would be successful. As a start, testing a greater number of subjects could strengthen the results of this study. Also, subjects with different degrees of high frequency hearing loss could be tested, provided that they still had DPOAEs at some frequencies. It would be interesting to observe what intensity of ultrasound would be required in order for them to perceive the tone, as well as to suppress their DPOAES. Additionally, these tests were conducted with a 30-kHz ultrasonic tone; other ultrasonic frequencies could be experimented with. However, previous studies have not found that the frequency of the ultrasound had a significant impact on perception (such as in Nishimura's 2003 study).

The scope of this study could also be expanded upon with other forms of testing. Psychoacoustical masking tests, similar to what was done by Nishimura, could be performed on the same test subjects that were used for this study, and resulting masking curves could be compared with their DPOAE suppression curves. Another type of objective testing would be Auditory Brainstem Response (ABR), in which the subject's neuronal action potentials are monitored by electrodes placed on the scalp in response to auditory stimuli, in order to determine if there is an impact on the signal being sent to the brain via the auditory nerve. This trio of testing (psychoacoustical, DPOAE and ABR) could provide a comprehensive picture of the impacts on these test subjects.

The same subjects could also participate in pitch-matching exercises, in which they are presented with a bone-conducted ultrasonic tone and a controllable air-conducted tone. The subject would adjust the air-conducted tone until it matched their perception of the bone-conducted ultrasonic tone.

Provided that this further testing continues to support the conclusions stated here, an important application of bone-conducted ultrasound is as an alternative hearing aid technology, through the use of amplitude modulation on an ultrasonic carrier frequency. Candidates would have significant high frequency hearing loss and middle ear disorders. As well, bone-conducted ultrasound is currently being used as a type of treatment for people suffering from tinnitus. Furthering the knowledge about bone-conducted ultrasound could provide some insight into the role of the inner ear in tinnitus and the ability to provide better treatment.

10 References

Deatherage, B.H., Jeffress, L.A., Blodgett, H.C. (1954): A note on the audibility of intense ultrasonic sound. *Journal of the Acoustical Society of America*, Vol. 26, No. 4, 1954, p. 582.

Dieroff, H.G., Ertel, H. (1975): Some thoughts on the perception of ultrasonics by man. *European Archives of Oto-Rhino-Laryngology*, Vol. 209, No. 4, 1975, pp. 277-290.

Dobie, R.A., Wiederhold, M.L. (1992): Ultrasonic hearing. *Science*, Vol. 255, 1992, p. 1584.

Dreisbach, L.E., Siegel, J.H. (2001): Distortion-product otoacoustic emissions measured at high frequencies in humans. *Journal of the Acoustical Society of America*, Vol. 110, No. 5, 2001, pp. 2456-2469.

Dreisbach, L.E., Long, K.M., Lees, S.E. (2006): Repeatability of high-frequency distortion-product otoacoustic emissions in normal-hearing adults. *Ear & Hearing*, Vol. 27, No. 5, 2006, pp. 466-479.

Encyclopaedia Britannica, Inc. (1997): Human Ear. *Encyclopaedia Britannica*, 2011, http://www.britannica.com/EBchecked/topic/175622/human-ear.

Fettiplace, R., Hackney, C.M. (2006): The sensory and motor roles of auditory hair cells. *Nature Reviews Neuroscience*, Vol. 7, January 2006, pp. 19-29.

Gorga, M.P., Neely, S.T., et al. (2003): Distortion product otoacoustic emission suppression tuning curves in normal-hearing and hearing-impaired human ears. *Journal of the Acoustical Society of America*, Vol. 114, No. 1, 2003, pp. 263-278.

Haeff, A.V., Knox, C. (1962): Perception of ultrasound. *Science*, Vol. 139, 1963, pp. 590-592.

Kemp, D.T. (2002): Otoacoustic emissions, their origin in cochlear function, and use. *British Medical Bulletin 2002*, Vol. 63, 2002, pp. 223-241.

Lenhardt, M.L., Skellett, R., et al. (1992): Human ultrasonic speech perception. *Science*, Vol. 253, 1991, pp. 82-85.

Neely, S., Liu, Z. (2001): *EMAV: Otoacoustic emission averager*. Technical Memorandum. Boys Town National Research Hospital, Omaha, USA, 26 pp.

Nishimura, T., Nakagawa, S., et al. (2003): Ultrasonic masker clarifies ultrasonic perception in man. *Hearing Research*, Vol. 175, 2003, pp. 171-177.

Ohyama, K., Kusakari, J., Kawamoto, K. (1985): Ultrasonic electrocochleography in guinea pig. *Hearing Research*, Vol. 17, 1985, pp. 143-151.

Pumphrey, R.J. (1950): Upper limit of frequency for human hearing. *Nature*, Vol. 166, 1950, p. 571.

Appendix A Matlab code for DPOAE tests

```
% Distortion Product OAE test for ultrasonic hearing study
% Created by Jennifer Martin-Roff and Ben Sheffield

clear all

%%%%%%%%%%     Begin Parameter Initialization Section     %%%%%%%%%%

%%%SYSTEM PARAMETERS%%%
Fs = 96000;         %sample rate is 96 kHz
sweeps = 16;        %# of sweeps (total recording buffers per set)
sets = 16;           %# of times primary pair is repeated (must be even);
buf_size = 4096;    %# of samples per sweep (recording buffer size)
gap_btwn_sets = 0.200;  %silence between sets (seconds)
% bcu_cf = 30000; % Ultrasonic frequency
Tonoffset = .200; % BCU offset from primary tones for on/off

%%%STIMULUS PARAMETERS%%%
f2 = [2; 4; 6; 8; 9; 10; 11; 12; 13; 14; 15; 16];  %f2 frequencies (kHz)
f2_f1_ratio = 1.2;      %ratio to calculate f1 from f2
L1_SPL = 57;    %desired f1 level (dB SPL)
L2_SPL = 45;    %desired f2 level (dB SPL)

%%% NOISE FLOOR DECISION PARAMETERS %%%
nnsb = 10;      %number of noise side bands (# of samples on either side of DP to
calculate noise floor)
nf_max = -15;   %maximum allowable noise floor
max_repeat = 2; %maximum number of times the tone pair will be repeated

%%%DISPLAY PARAMETERS%%%
fmin=20;   %min abscissa (Hz)
fmax=40000; %max abscissa (Hz)

%%%CALIBRATION PARAMETERS SDSU%%%
DA1_sens = 0.3226;  %cnt_0toPk / Vrms
DA2_sens = 0.3226;  %cnt_0toPk / Vrms
transducer_sens = 112;  %SPL/Vrms; ER-2s = 100; CX-300s = 112;
L = 84;         %cnt adjustment for transducer 1
R = 124;        %cnt adjustment for transducer 2
AD_sens = 0.0598;   %cnt_rms / Vrms
probe_sens = 1.75;  %probe mic sensitivity (V/Pa)

%%%%%%%%%%     End Parameter Initialization Section     %%%%%%%%%%


%%%%%%%%%%     Begin Stimulus Definition Section     %%%%%%%%%%

f2 = f2*1000;   %convert to Hz
num_tones = length(f2);  %number of tone pairs presented

% randomize order of frequency sweep (down by default)
if rand < 0.5
    f2 = flipud(f2) %sweep up
end

f1 = f2/f2_f1_ratio;                    %calculate f1 primary tones (Hz)

risetime = 0.01; % ramp up 10 msec
fcr = (acos(-1)-acos(1))/(2*pi*risetime);
x = 1:round(risetime*Fs);
crr = (0.5+cos(pi+2*pi*fcr*x/Fs)/2)'; %onset
crf = (0.5+cos(2*pi*fcr*x/Fs)/2)'; %offset

%%% Load EMAV Calibration file and adjust L1 and L2 values %%%
cal_filename = get(findobj('tag','cal_file'),'string');  %Get EMAV Calibration File
Name from GUI
[cal_freq_scale,cal_L,cal_R,val_1k_L,val_1k_R] = cal2mat(cal_filename);

cal_tones_L = spline(cal_freq_scale*1000,cal_L,f2);
cal_tones_R = spline(cal_freq_scale*1000,cal_R,f1);
Loffset = cal_tones_L - val_1k_L;
Roffset = cal_tones_R - val_1k_R;
```

```
L2_SPL_correct = L2_SPL - Loffset; % Corrected L2 in dBSPL
L1_SPL_correct = L1_SPL - Roffset;

L2_V = 10.^((L2_SPL_correct-transducer_sens)/20);    %convert from desired SPL to
Volts for Sennheiser CX-300
L1_V = 10.^((L1_SPL_correct-transducer_sens)/20);    %convert from desired SPL to
Volts for Sennheiser CX-300
L2 = DA1_sens*L*L2_V;     %level of test tone 1 (cnt)
L1 = DA2_sens*R*L1_V;     %level of test tone 2 (cnt)

for m=1:num_tones
    if L2(num_tones+1-m,1) >= 1
        L2(num_tones+1-m,1) = 0.999;
        disp(['L2 saturated at : ' num2str(f2(num_tones+1-m,1))])
    end
    if L1(num_tones+1-m,1) >= 1
        L1(num_tones+1-m,1) = 0.999;
        disp(['L1 saturated at : ' num2str(f1(num_tones+1-m,1))])
    end
end

prim_dur = sweeps*buf_size;     %primary tone duration (samples)
prim_dur_sec = prim_dur/Fs;    %primary tone duration (seconds)
T = 0:1/Fs:prim_dur_sec-1/Fs;   %period of each primary tone set

bcu_dur_sec = prim_dur_sec+2*Tonoffset; %Ultrasonic tone duration (sec)
bcu_dur = bcu_dur_sec*Fs; %Ultrasonic tone duration (samples)
t_bcu = 0:1/Fs:bcu_dur_sec-1/Fs; %period of each ultrasonic tone set

t_bcu_onoffset = zeros(round(Tonoffset*Fs),2);


%%%%%%%%%%  Open audio channels

ao1 = analogoutput('winsound',5); % 5 = lab, 0 = home
addchannel(ao1,1:2);
set(ao1,'StandardSampleRates','Off');
ao1_props = propinfo(ao1, 'SampleRate');
set(ao1,'SampleRate',Fs);

ao2 = analogoutput('winsound',4); % 5 = lab, 0 = home
addchannel(ao2,1:2);
set(ao2,'StandardSampleRates','Off');
ao2_props = propinfo(ao2, 'SampleRate');
set(ao2,'SampleRate',Fs);

ai = analoginput('winsound',4); % 4 = lab, 0 = home
addchannel(ai,1);
set(ai,'StandardSampleRates','Off');
ai_props = propinfo(ai, 'SampleRate');
set(ai,'SampleRate',Fs)

set([ai ao1 ao2],'TriggerType','Manual')
set(ai,'ManualTriggerHwOn','Trigger')

%%%Initialize Data%%%
DPgram = []; %DPgram starts out blank
DPgram_scale = []; %DPgram scale starts blank
f1_levels = [];
f2_levels = [];
nf_levels = [];
resp_per_pair=[];
nf_per_pair=[];
repeat_tp = 0;

%%% START LOOP %%%
%Create primary tones
i=1;
while i <= num_tones
    tonef2 = sin(2*pi*f2(num_tones+1-i)*T)';
    tonef2(1:length(crr)) = tonef2(1:length(crr)).*crr;
    tonef2((end-length(crf)+1):end) = tonef2((end-length(crf)+1):end).*crf;
    tonef2 = L2(num_tones+1-i)*tonef2;

    tonef1 = sin(2*pi*f1(num_tones+1-i)*T)';
    tonef1(1:length(crr)) = tonef1(1:length(crr)).*crr;
```

```
    tonef1((end-length(crf)+1):end) = tonef1((end-length(crf)+1):end).*crf;
    tonef1 = L1(num_tones+1-i)*tonef1;

    bcu_cf = 1000*str2num(get(findobj('tag','cf_mask'),'string'));
    BCU_Level = str2num(get(findobj('tag','BCU_Level'),'string'));
    tonesupp = sin(2*pi*bcu_cf*t_bcu)';
    tonesupp(1:length(crr)) = tonesupp(1:length(crr)).*crr;
    tonesupp((end-length(crf)+1):end) = tonesupp((end-length(crf)+1):end).*crf;
    tonesupp = 10^(BCU_Level/20).*tonesupp;

    empty = zeros(length(tonesupp),1);

    tonesupp = [tonesupp empty];

    set_gap = zeros(gap_btwn_sets*Fs,2);

    y1 = [t_bcu_onoffset; tonef2 tonef1; t_bcu_onoffset; set_gap; ...
          t_bcu_onoffset; tonef2 tonef1; t_bcu_onoffset; set_gap; ...
          t_bcu_onoffset; tonef2 tonef1; t_bcu_onoffset; set_gap; ...
          t_bcu_onoffset; tonef2 tonef1; t_bcu_onoffset; set_gap; ...
          t_bcu_onoffset; tonef2 tonef1; t_bcu_onoffset; set_gap; ...
          t_bcu_onoffset; tonef2 tonef1; t_bcu_onoffset; set_gap; ...
          t_bcu_onoffset; tonef2 tonef1; t_bcu_onoffset; set_gap; ...
          t_bcu_onoffset; tonef2 tonef1; t_bcu_onoffset; set_gap; ...
          t_bcu_onoffset; tonef2 tonef1; t_bcu_onoffset; set_gap; ...
          t_bcu_onoffset; tonef2 tonef1; t_bcu_onoffset; set_gap; ...
          t_bcu_onoffset; tonef2 tonef1; t_bcu_onoffset; set_gap; ...
          t_bcu_onoffset; tonef2 tonef1; t_bcu_onoffset; set_gap; ...
          t_bcu_onoffset; tonef2 tonef1; t_bcu_onoffset; set_gap; ...
          t_bcu_onoffset; tonef2 tonef1; t_bcu_onoffset; set_gap; ...
          t_bcu_onoffset; tonef2 tonef1; t_bcu_onoffset; set_gap; ...
          t_bcu_onoffset; tonef2 tonef1; t_bcu_onoffset];

    y2 = [tonesupp; set_gap; tonesupp; set_gap; ...
          tonesupp; set_gap; tonesupp; set_gap; ...
          tonesupp; set_gap; tonesupp; set_gap; ...
          tonesupp; set_gap; tonesupp; set_gap; ...
          tonesupp; set_gap; tonesupp; set_gap; ...
          tonesupp; set_gap; tonesupp; set_gap; ...
          tonesupp; set_gap; tonesupp; set_gap; ...
          tonesupp; set_gap; tonesupp];

    set(ai, 'SamplesPerTrigger', length(y2))

    putdata(ao1,y1)
    putdata(ao2,y2)
    start([ai ao1 ao2])
    trigger([ai ao1 ao2])

%     aitime = ai.InitialTriggerTime;
%     aotime = get(ao,'InitialTriggerTime');
%     delay = aitime(6) - aotime(6);
%     delay = round(0.02*Fs);

    wait(ao2,length(y2))
    recorded_data = getdata(ai);


%%%%%%%%%%%%%%%%%%%%%%%%%%%%%%%%%%%%%%%%%%%%%%%%%%%%%%%%%%%%%%%%%%%%%%%%%%%%%%%%%%%%%%%%%%
%%%%%%%%%%

    %%%%%%%%%%     Begin Response Analysis Section     %%%%%%%%%%

    % Section the recorded sets into sweep segments (time domain)
    resp_avg_t=[];     %initiate response average per sweep (time domain)
    noise_est_t=[];    %initiate noise floor estimate per sweep (time domain)

    recorded_data = recorded_data/AD_sens;      %convert from cnt to V
    recorded_data = recorded_data/probe_sens;   %convert from V to Pa

    gap = length(set_gap);
    onoffset = length(t_bcu_onoffset);

    resp_set1 = recorded_data(1*onoffset+0*(prim_dur+gap)+1 :
1*onoffset+1*prim_dur+0*gap,1);
    resp_set2 = recorded_data(3*onoffset+1*(prim_dur+gap)+1 :
3*onoffset+2*prim_dur+1*gap,1);
```

```
    resp_set3 = recorded_data(5*onoffset+2*(prim_dur+gap)+1 :
5*onoffset+3*prim_dur+2*gap,1);
    resp_set4 = recorded_data(7*onoffset+3*(prim_dur+gap)+1 :
7*onoffset+4*prim_dur+3*gap,1);
    resp_set5 = recorded_data(9*onoffset+4*(prim_dur+gap)+1 :
9*onoffset+5*prim_dur+4*gap,1);
    resp_set6 = recorded_data(11*onoffset+5*(prim_dur+gap)+1 :
11*onoffset+6*prim_dur+5*gap,1);
    resp_set7 = recorded_data(13*onoffset+6*(prim_dur+gap)+1 :
13*onoffset+7*prim_dur+6*gap,1);
    resp_set8 = recorded_data(15*onoffset+7*(prim_dur+gap)+1 :
15*onoffset+8*prim_dur+7*gap,1);
    resp_set9 = recorded_data(17*onoffset+8*(prim_dur+gap)+1 :
17*onoffset+9*prim_dur+8*gap,1);
    resp_set10 = recorded_data(19*onoffset+9*(prim_dur+gap)+1 :
19*onoffset+10*prim_dur+9*gap,1);
    resp_set11 = recorded_data(21*onoffset+10*(prim_dur+gap)+1 :
21*onoffset+11*prim_dur+10*gap,1);
    resp_set12 = recorded_data(23*onoffset+11*(prim_dur+gap)+1 :
23*onoffset+12*prim_dur+11*gap,1);
    resp_set13 = recorded_data(25*onoffset+12*(prim_dur+gap)+1 :
25*onoffset+13*prim_dur+12*gap,1);
    resp_set14 = recorded_data(27*onoffset+13*(prim_dur+gap)+1 :
27*onoffset+14*prim_dur+13*gap,1);
    resp_set15 = recorded_data(29*onoffset+14*(prim_dur+gap)+1 :
29*onoffset+15*prim_dur+14*gap,1);
    resp_set16 = recorded_data(31*onoffset+15*(prim_dur+gap)+1 :
31*onoffset+16*prim_dur+15*gap,1);

    for j=1:sweeps-1 % (throw out first sweep, j = 1)
        A_seg = resp_set1(j*buf_size+1:j*buf_size+buf_size)';
        B_seg = resp_set2(j*buf_size+1:j*buf_size+buf_size)';
        C_seg = resp_set3(j*buf_size+1:j*buf_size+buf_size)';
        D_seg = resp_set4(j*buf_size+1:j*buf_size+buf_size)';
        E_seg = resp_set5(j*buf_size+1:j*buf_size+buf_size)';
        F_seg = resp_set6(j*buf_size+1:j*buf_size+buf_size)';
        G_seg = resp_set7(j*buf_size+1:j*buf_size+buf_size)';
        H_seg = resp_set8(j*buf_size+1:j*buf_size+buf_size)';
        I_seg = resp_set9(j*buf_size+1:j*buf_size+buf_size)';
        J_seg = resp_set10(j*buf_size+1:j*buf_size+buf_size)';
        K_seg = resp_set11(j*buf_size+1:j*buf_size+buf_size)';
        L_seg = resp_set12(j*buf_size+1:j*buf_size+buf_size)';
        M_seg = resp_set13(j*buf_size+1:j*buf_size+buf_size)';
        N_seg = resp_set14(j*buf_size+1:j*buf_size+buf_size)';
        O_seg = resp_set15(j*buf_size+1:j*buf_size+buf_size)';
        P_seg = resp_set16(j*buf_size+1:j*buf_size+buf_size)';

        resp_avg_t = [resp_avg_t;
(A_seg+B_seg+C_seg+D_seg+E_seg+F_seg+G_seg+H_seg+I_seg+J_seg+K_seg+L_seg+M_seg+N_seg+O
_seg+P_seg)/16];     %Time average corresponding sweeps from each set to estimate
response
        noise_est_t = [noise_est_t; (A_seg-B_seg+C_seg-D_seg+E_seg-F_seg+G_seg-
H_seg+I_seg-J_seg+K_seg-L_seg+M_seg-N_seg+O_seg-P_seg)/16];     %Subtract
corresponding sweeps from each set to estimate noise floor
    end

    %This section sets the reference for dBSPL
    wref = flattopwin(buf_size);
    T_ref = 0:1/buf_size:1-1/buf_size;   %1 sweep reference block
    p_ref_rms = 20e-6;      %20 uPa rms for 0dB ref amplitude
    p_ref_0topk = p_ref_rms*sqrt(2);    %zero to peak amplitude of pressure wave
    x_ref = p_ref_0topk*sin(2*pi*1000*T_ref)';   %0 dB reference is 1 kHz pure tone
    X_ref = fft(wref.*x_ref);     %take fft of reference signal
    Xmag_ref = abs(X_ref);  %magnitude of reference signal
    Xdb_ref = 20*log10(Xmag_ref);   %convert to dB scale
    Xdb_ref = max(Xdb_ref);     %take max amplitude as 0dB reference for fft
    %end reference section

    %Define frequency scale for display
    freq_res = Fs/buf_size;
    freq_scale = freq_res*(0:buf_size/2);
    smin=floor(fmin/freq_res)+1;
    smax=floor(fmax/freq_res)+1;
    freq_scale = freq_scale(smin:smax)'/1000; %Since freq_scale(1) is 0, we need to
add 1 to the index

    % Transform sweep segments into frequency domain
```

```
    resp_avg_f=[];     %initiate response average per sweep (freq domain)
    noise_est_f=[];    %initiate noise floor estimate per sweep (freq domain)
    w = flattopwin(buf_size);
    for m=1:sweeps-1
        RESP = fft(w.*resp_avg_t(m,:)');
        RESP = abs(RESP);
        RESP = 20*log10(RESP)';
        RESP_db_corr = RESP(smin:smax);
        RESP_dbSPL = RESP_db_corr - Xdb_ref;
        resp_avg_f = [resp_avg_f; RESP_dbSPL];

        NF = fft(w.*noise_est_t(m,:)');
        NF = abs(NF);
        NF = 20*log10(NF)';
        NF_db_corr = NF(smin:smax);
        NF_dbSPL = NF_db_corr - Xdb_ref;
        noise_est_f = [noise_est_f; NF_dbSPL];
    end

    % Average fft results across sweeps
    grand_resp_avg = sum(resp_avg_f)/(size(resp_avg_f,1));
    grand_nf_avg = sum(noise_est_f)/(size(noise_est_f,1));

    grand_resp_corr = grand_resp_avg;  %no mic correction
    grand_nf_corr = grand_nf_avg;   %no mic correction

    % Plot corrected frequency response (blue) and noise floor (green)
    figure
    plot(freq_scale,grand_resp_corr,freq_scale,grand_nf_corr)
    axis([0 20 -40 70])
    title(['Frequency content of DPOAE Response   f2=' num2str(f2(num_tones+1-i)) '
f1=' num2str(f1(num_tones+1-i)) ])
    xlabel('Frequency (kHz)')
    ylabel('dB SPL')

    %%% MEASURE PRIMARY, DP, AND NF LEVELS AND PLOTS THE DP GRAM

    %Check for distortion product at 2f1-f2
    DP_freq = 2*f1(num_tones+1-i)-f2(num_tones+1-i);
    DP_sample = round((DP_freq - fmin)/freq_res)+1;
    DP_level = grand_resp_corr(DP_sample);
    % DP_level_max = max(grand_resp_corr(DP_sample-5:DP_sample+5));

    NFatDP_max = mean(grand_nf_corr(DP_sample-nnsb:DP_sample+nnsb));

    if NFatDP_max <= nf_max
        nf_levels = [NFatDP_max; nf_levels];
        DPgram = [DP_level ; DPgram];
        DPgram_scale = [f2(num_tones+1-i)/1000 ; DPgram_scale];

        f1_sample = round((f1(num_tones+1-i) - fmin)/freq_res)+1;
        f1_levels = [grand_resp_corr(f1_sample) ; f1_levels];
        f2_sample = round((f2(num_tones+1-i) - fmin)/freq_res)+1;
        f2_levels = [grand_resp_corr(f2_sample) ; f2_levels];

        figure(2)
        plot(DPgram_scale,f1_levels,'-b+',DPgram_scale,f2_levels,'-
m+',DPgram_scale,DPgram,'xr-',DPgram_scale,nf_levels,'ks-')
        axis([0 20 -40 70])
        title('DP-gram')
        xlabel('Frequency (kHz)')
        ylabel('dB SPL')
        legend('f1','f2','DP levels','Noise Floor','Location','NorthEast')

        resp_per_pair = [resp_per_pair; grand_resp_corr];
        nf_per_pair = [nf_per_pair; grand_nf_corr];

        i = i+1;
        repeat_tp = 0;
    else
        repeat_tp = repeat_tp+1;
        if repeat_tp >= max_repeat
            i=i+1;
        end
    end
    pause(18.0)
end
```

```
%%% end while loop %%%

%%% Save data with date-coded and sequential filenaming system %%%
dataname = [cal_filename(1:end-4)];
iter = str2num(dataname(end-1:end));
checkfile=1;
while checkfile
    if exist([dataname '.mat']) == 2
        iter = iter+1;
        if iter < 10
            dataname = [dataname(1:end-2) '0' num2str(iter)];
        else
            dataname = [dataname(1:end-2) num2str(iter)];
        end
    else checkfile = 0;
    end
end

bcu_MCL = str2num(get(findobj('tag','BCU_MCL'),'string'));
bcu_th = str2num(get(findobj('tag','BCU_SL'),'string'));
bcu_dBSL = str2num(get(findobj('tag','dB_mask'),'string'));
save(dataname,
'cal_filename','f1','f2','L1_SPL','L2_SPL','L1_V','L2_V','Fs','sweeps','sets','buf_siz
e','f2_f1_ratio','num_tones', ...

'freq_scale','resp_per_pair','nf_per_pair','DPgram_scale','DPgram','nf_levels','f1_lev
els','f2_levels','bcu_MCL','bcu_th','bcu_dBSL');

delete(ai)
clear ai
delete(ao1)
clear ao1
delete(ao2)
clear ao2
```

Appendix B Input Panel for DPOAE tests